High temperature strain glass in Ti-Au and Ti-Pt based shape memory alloys

Shuai Ren(任帅), Chang Liu(刘畅), and Wei-Hua Wang(汪卫华)

Citation: Chin. Phys. B, 2021, 30 (**1**): 018101. DOI: 10.1088/1674-1056/abc54a
Journal homepage: http://cpb.iphy.ac.cn; http://iopscience.iop.org/cpb

What follows is a list of articles you may be interested in

LaGa-based bulk metallic glasses

Lin-Zhi Zhao(赵林志), Rong-Jie Xue(薛荣洁), Wei-Hua Wang(汪卫华), Hai-Yang Bai(白海洋)
Chin. Phys. B, 2017, 26 (**1**): 018106. DOI: 10.1088/1674-1056/26/1/018106

Evolution of magnetic domain structure of martensite in Ni-Mn-Ga films under the interplay of the temperature and magnetic field

Xie Ren, Wei Jun, Liu Zhong-Wu, Tang Yan-Mei, Tang Tao, Tang Shao-Long, Du You-Wei
Chin. Phys. B, 2014, 23 (**6**): 068103. DOI: 10.1088/1674-1056/23/6/068103

Relation between martensitic transformation temperature range and lattice distortion ratio of NiMnGaCoCu Heusler alloys

Wei Jun, Xie Ren, Chen Le-Yi, Tang Yan-Mei, Xu Lian-Qiang, Tang Shao-Long, Du You-Wei
Chin. Phys. B, 2014, 23 (**4**): 048107. DOI: 10.1088/1674-1056/23/4/048107

Thermal stability and high-temperature shape memory characteristics of Ti-20Zr-10Ta alloy

Zheng Xiao-Hang, Sui Jie-He, Zhang Xin, Yang Zhe-Yi, Cai Wei
Chin. Phys. B, 2014, 23 (**1**): 018101. DOI: 10.1088/1674-1056/23/1/018101

Magnetostructural transition in NiCuCoMnGa alloys

Li Pan-Pan, Wang Jing-Min, Jiang Cheng-Bao
Chin. Phys. B, 2013, 22 (**8**): 088105. DOI: 10.1088/1674-1056/22/8/088105

RAPID COMMUNICATION

High temperature strain glass in Ti–Au and Ti–Pt based shape memory alloys*

Shuai Ren(任帅)[1,†], Chang Liu(刘畅)[2], and Wei-Hua Wang(汪卫华)[1,‡]

[1] Institute of Physics, Chinese Academy of Sciences, Beijing 100190, China

[2] Frontier Institute of Science and Technology, State Key Laboratory for Mechanical Behavior of Materials, Xi'an Jiaotong University, Xi'an 710049, China

(Received 8 September 2020; revised manuscript received 10 October 2020; accepted manuscript online 28 October 2020)

Strain glass is a frozen short-range strain ordered state found in shape memory alloys recently, which exhibits novel properties around the ideal glass transition temperature T_0. However, the T_0 of current strain glass systems is still very low, limiting their potential applications and experimental studies. In this paper, we reported two new strain glass systems with relatively high T_0. In $Ti_{50}Au_{50-x}Cr_x$ alloys, the strain glass appears at $x = 25$, and exhibits a T_0 of 251 K, while in $Ti_{50}Pt_{50-y}Fe_y$ alloys, the strain glass takes place at $y = 30$, and shows a T_0 of 272 K. Both of them are comparable with the highest T_0 value reported so far. Moreover, the phase diagrams of main strain glass systems in Ti-based alloys were summarized. It is found that the influence of the martensitic transformation temperature of the host alloy on the T_0 of the strain glass is limited. This work may help to design new strain glass systems with higher T_0 above ambient temperature.

Keywords: shape memory alloys, martensitic transformation, strain glass, glass transition temperature

PACS: 81.30.Kf, 81.30.Bx **DOI:** 10.1088/1674-1056/abc54a

1. Introduction

Shape memory alloys (SMAs) are one of the most important smart materials that exhibit unique properties of the shape memory effect and superelasticity, due to a ferroelastic/martensitic transformation.[1] The two main SMA systems for current commercial applications are Ti–Ni-based and Cu-based alloys.[1] However, their martensitic transformation temperatures (M_s) are generally lower than 373 K, which limits the applications of SMAs in high temperature conditions. As a result, Ti–Au and Ti–Pt high temperature SMAs (HTSMAs) have received wide attention due to their high M_s.[2–4]

Doping is an essential way to modify the martensitic transformation as well as the associated properties in SMAs.[5] However, doping usually introduces point defects into the SMAs, and thus further reduces the M_s. In recent years, it has been reported that when the martensitic transformation in SMAs is suppressed by excess doping, the system does not directly become nontransforming, but exhibits a novel glass transition.[6] As a result, the long-range strain ordered phase (i.e., martensitic phase) is replaced by a short-range strain ordered glass state, which is termed as the "strain glass" given that the lattice strain is the order parameter of the martensitic transformation.[6]

Strain glass is characterized by several typical features, such as no enthalpy change during the glass transition observed by differential scanning calorimetry (DSC), the disappearance of thermal hysteresis in electrical resistivity curves, and no breaking of the parent phase symmetry during the glass transition in the x-ray diffraction spectrums.[7] It also exhibits some important glass transition features, including the dynamic freezing measured by dynamic mechanical analysis (DMA) experiments and the breaking down of ergodicity measured by zero-field-cooling and field-cooling (ZFC/FC) experiments.[7] Moreover, the strain glass is of potential interest for applications, because it exhibits many interesting properties, such as the superelasticity of slim hysteresis,[8] stress tuned intelligent damping properties,[9] and low-field-triggered large magnetostriction.[10] Unfortunately, the glass transition temperature (T_g) of current strain glass alloys is generally lower than 273 K, which not only limits the potential applications of the strain glass, but also interrupts the investigation of the nature of strain glass as well.

For example, the low glass transition temperature makes the experimental investigation of dynamic relaxation of strain glass difficult. Dynamic relaxation is an intrinsic feature of glasses, and exploring the dynamic relaxation of glasses is significant for understanding the nature of glasses.[11] The dynamic relaxation is generally measured by the DMA experiments, and the lower temperature limit of the DMA is around 130 K, as illustrated in Fig. 1. In metallic glass, thanks to their high T_g, several unique dynamic relaxation modes are observed, including primary α-relaxation, β-relaxation, and

*Project supported by China Postdoctoral Science Foundation (Grant No. 2019M650880), the National Natural Science Foundation of China (Grant Nos. 51901243, 61888102, and 11790291), the Natural Science Foundation of Guangdong Province, China (Grant No. 2019B030302010), and the Strategic Priority Research Program of the Chinese Academy of Sciences (Grant No. XDB30000000).

†Corresponding author. E-mail: shuai.ren@iphy.ac.cn

‡Corresponding author. E-mail: whw@iphy.ac.cn

nearly constant loss, as illustrated in the loss modulus curve of a $La_{55}Ni_{20}Al_{25}$ bulk metallic glass (BMG) in Fig. 1(a). In comparison, only one relaxation mode has been reported in strain glass up to now.[6,7] As shown in Fig. 1(b), there is a peak in the loss modulus curve of a $Ti_{48.5}Ni_{51.5}$ strain glass alloy, close to the lower temperature limit of the DMA, which corresponds to the primary α-relaxation of the BMG. No other relaxation mode can be found except this peak, due to the low T_g of the strain glass.

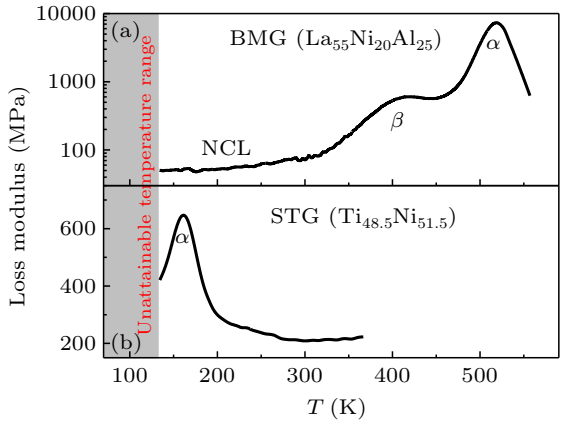

Fig. 1. Comparison of the loss modulus curve of (a) a $La_{55}Ni_{20}Al_{25}$ bulk metallic glass (BMG) and (b) a $Ti_{48.5}Ni_{51.5}$ strain glass (STG) alloy, measured by the DMA experiment. The lower temperature limit is around 130 K. Above this limit, the BMG exhibits several relaxation modes in (a), including primary α-relaxation mode, β-relaxation mode, and nearly constant loss (NCL), while the strain glass only exhibits one α-relaxation mode in (b).

In metallic glass, the β-relaxation has been well known as one of the intrinsic dynamic relaxation modes besides the α-relaxation, which corresponds to localized cooperative motions of a small number of atoms confined in loosely packed regions.[11] If strain glass possesses the same glassy dynamics as metallic glass, the β-relaxation should exist in the strain glass in principle. Therefore, the investigation of possible β-relaxation in strain glass may provide insight into the common dynamic characteristics of these two glasses, and deepen the understanding of the nature of strain glass. However, the investigation is interrupted due to the low T_g of current strain glass systems. As a result, it is of importance to discover high temperature strain glass systems.

In $Ti_{50}Ni_{50x}Fe_x$ SMAs, the T_g of strain glass at $x = 6$ is around 180 K, while the M_s of the host alloy (i.e., $Ti_{50}Ni_{50}$) is around 350 K.[12] On the other hand, in $Ti_{50}Pd_{50-x}Fe_x$ SMAs, the T_g of strain glass at $x = 14$ is about 280 K, while the M_s of the host alloy (i.e., $Ti_{50}Pd_{50}$) is around 800 K.[13] The comparison between these two systems gives us a clue that the strain glass with high T_g comes from high M_s SMA systems. Therefore, we chose the two HTSMAs, $Ti_{50}Au_{50}$ ($M_s = 893$ K) and $Ti_{50}Pt_{50}$ ($M_s = 1340$ K),[2] as the host alloys and tried to find the strain glass in them. In this paper, we reported the strain glass with relatively high T_g found in these two HTSMAs. In $Ti_{50}Au_{50-x}Cr_x$ SMAs, strain glass appears at $x = 25$, while in $Ti_{50}Pt_{50-y}Fe_y$ SMAs, strain glass takes place at $y = 30$. Owing to the very high M_s of the host alloys, these two systems both exhibit a relatively large ideal glass transition temperature (T_0), which is comparable with the highest T_0 value reported until now.

2. Experimental methods

Samples of $Ti_{50}Au_{50-x}Cr_x$ ($x = 15$, 25, abbreviated by Crx hereafter) and $Ti_{50}Pt_{50-y}Fe_y$ ($y = 25$, 30, abbreviated by Fey hereafter) alloys were prepared from highly pure metals (> 99.95 at.%) by arc-melting under an argon atmosphere. The ingots were solution-treated at 1373 K for 12 h in evacuated quartz tubes, followed by water quenching. Then the ingots were cut into suitable shapes for different measurements. Latent heat of transformation was measured with a differential scanning calorimeter (DSC-Q200 from TA Company) with a cooling/heating rate of 10 K/min. Electrical resistivity (ER) of specimens was measured through a four-probe method with a constant current of 100 mA and a cooling/heating rate of 2 K/min. The anelasticity was detected by dynamic mechanical analysis (DMA-Q800 from TA Instruments) using a cooling rate of 2 K/min with a single cantilever mode in the frequency range from 0.2 Hz to 20 Hz.

3. Results and discussion

Figures 2(a1) and 2(a2) exhibit the DSC curves of $Ti_{50}Au_{50-x}Cr_x$ SMAs. Sharp heat flow peaks are observed during cooling and heating for Cr15 of which the M_s is around 385 K, while the heat flow peaks disappear for Cr25. It means that 25 at.% of chromium is enough to suppress the martensitic transformation in Ti–Au SMAs. On the other hand, in $Ti_{50}Pt_{50-y}Fe_y$ SMAs, the doping of 25 at.% iron is still not high enough to lead to the suppression of the martensitic phase. As shown in Fig. 2(b1), weak heat flow peaks are detected for Fe25 ($M_s = 403$ K), while figure 2(b2) shows that it requires 30 at.% of iron to completely suppress the formation of the martensitic phase.

Figure 3 exhibits the ER curves with different doping levels for these two systems respectively. Because the martensitic transformation is the first order phase transformation in thermodynamics, it always exhibits a thermal hysteresis loop in the ER curve during cooling and heating. As shown in Fig. 3(a1), a clear thermal hysteresis loop takes place in the ER curve of Cr15, while no hysteresis loop is observed for Cr25 in Fig. 3(a2). It means that the martensitic transformation still exists in Cr15, whereas there is no martensitic transformation in Cr25. A similar case is found in $Ti_{50}Pt_{50-y}Fe_y$ SMAs. The absence of hysteresis loop in the ER curve of Fe30 in Fig. 3(b2) indicates that there is no martensitic transformation in Fe30 either. Thus, the ER curves are consistent with the

DSC results. Both of them indicate that the martensitic transformations in the two HTSMAs can be completely suppressed by doping excess point defects.

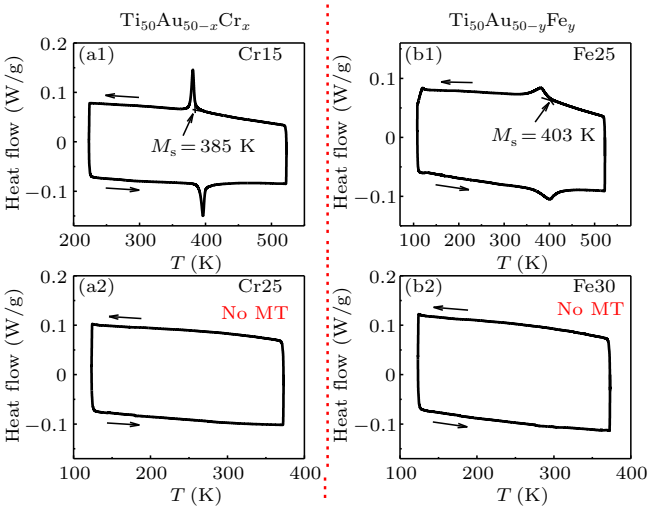

Fig. 2. DSC curves of $Ti_{50}Au_{50-x}Cr_x$ and $Ti_{50}Pt_{50-y}Fe_y$ alloys. Heat flow peaks can be observed in (a1) Cr15 and (b1) Fe25, while there is no peak in (a2) Cr25 and (b2) Fe30.

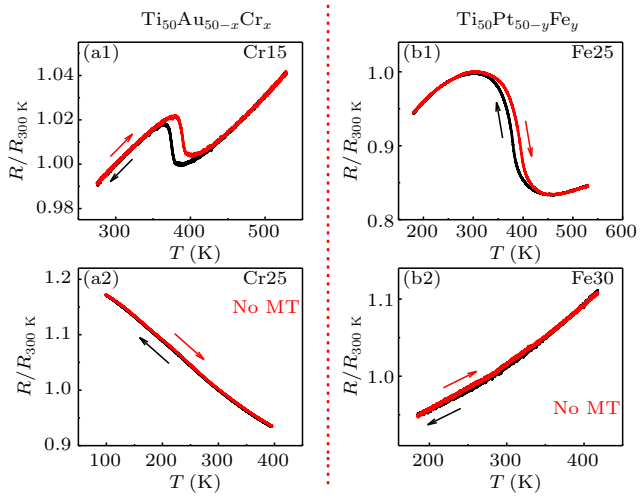

Fig. 3. ER curves of $Ti_{50}Au_{50-x}Cr_x$ and $Ti_{50}Pt_{50-y}Fe_y$ alloys. Thermal hysteresis loops can be observed in (a1) Cr15 and (b1) Fe25, while the hysteresis loop disappears in (a2) Cr25 and (b2) Fe30.

It is noted that the strain glass in Ti–Au–Cr alloys exhibits a negative temperature dependence of electrical resistivity in Fig. 3(a2), while the strain glass in Ti–Pt–Fe alloys shows a positive temperature dependence in Fig. 3(b2). The electrical resistivity has been well known to be sensitive to the phase structure of the nanodomains in strain glass.[12,14–16] Thus, the difference in the temperature dependence of electrical resistivity suggests that the phase structure of the nanodomains in these two strain glasses is remarkably different, which is worthy to be investigated in the future.

The storage modulus and tanδ curves of Cr25 and Fe30 are shown in Fig. 4 respectively. In Fig. 4(a), there are two anomalies in the storage modulus curves of Cr25 upon cooling. The first anomaly appears around 300 K, and exhibits a frequency dependent behavior, namely, the dip temperatures in storage modulus decrease with frequency lowering. Corresponding to the dip in storage modulus, the tanδ exhibits a peak, and the peak temperatures show the same frequency dependent behavior. This frequency dependent behavior is a typical glass feature for strain glass as previously reported, which indicates the slowing-down of dynamics during the strain glass transition.[6,7] It thus corresponds to the primary α-relaxation in metallic glass, as shown in Fig. 1(a). The frequency dependence of the dip can be fitted by the Vogel–Fulcher (V–F) relation $\omega = \omega_0 \exp[-E_a/k_B(T_g - T_0)]$,[6,7] where ω is the oscillating frequency, ω_0 the frequency at infinitely high temperature, E_a the activation energy, k_B the Boltzmann constant, T_g the strain glass transition temperature, and T_0 the ideal freezing temperature. For convenience, we use the T_0 to compare the glass transition temperatures of different systems below. According to the V–F relation, the ideal freezing temperature T_0 is about 251 K.

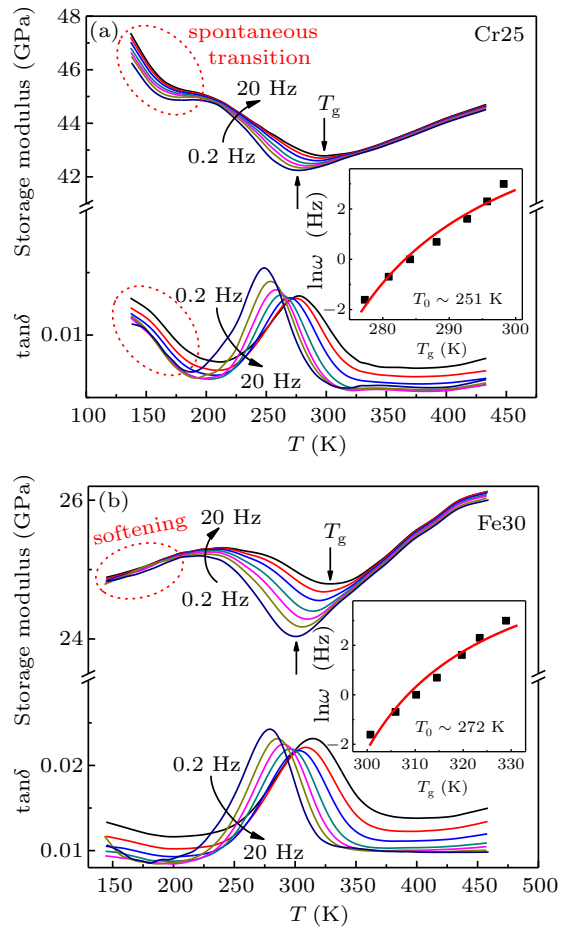

Fig. 4. (a) Storage modulus and tanδ curves of $Ti_{50}Au_{25}Cr_{25}$ (Cr25). Two anomalies are detected in the curves. The anomaly around 290 K exhibits a frequency dependent behavior, corresponds to the strain glass transition. By fitting the V–F relation in the inset of (a), the ideal freezing temperature T_0 is around 251 K. The other anomaly around 160 K in the storage modulus curve corresponds to a spontaneous transition from strain glass to martensite. (b) Storage modulus and tanδ curves of $Ti_{50}Pt_{20}Fe_{30}$ (Fe30). The anomaly around 320 K corresponds to the strain glass transition. According to the V–F relation in the inset of (b), the T_0 is around 272 K. Upon cooling, a modulus softening is observed at low temperatures.

With further cooling, another dip in the storage modulus curves of Cr25 appears around 150 K in Fig. 4(a). Meanwhile, the intensity of tanδ increases correspondingly, but the peak cannot be detected. This second anomaly indicates that a spontaneous transition from the strain glass (the frozen local strain ordered state) to martensite (the ferroelastic phase with long-range strain ordering) takes place. Such a spontaneous transition has been widely found in strain glass alloys,[17–19] which suggests that the strain glass is not the ground state of the system at low temperatures.

The storage modulus and tanδ curves of Fe30 are shown in Fig. 4(b). Only one anomaly is clearly found around 320 K, which exhibits the frequency dependent behavior of the dip temperatures in storage modulus and the corresponding peak temperatures in tanδ, the same as the first anomaly of Cr25. By fitting the V–F relation, T_0 is about 272 K. When the temperature further decreases, no second anomaly can be detected. Despite the absence of the second anomaly, the modulus softening is observed upon cooling below 230 K, which is known as a signal of the onset of the martensitic transition.[18] It suggests that the second anomaly actually exists, but locates at a low temperature below the lower limit of the DMA experiment. As a result, only the strain glass transition is clearly observed for Fe30 by the DMA experiment.

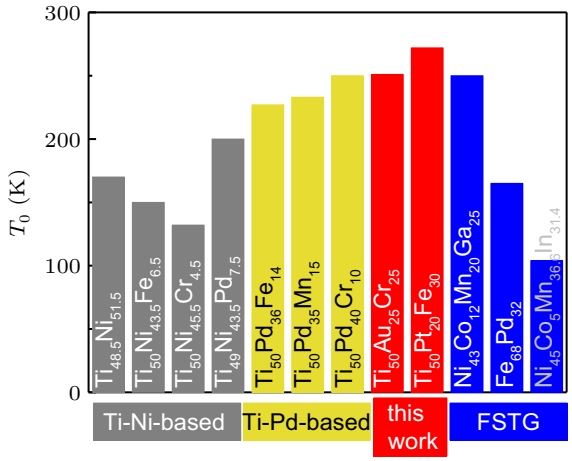

Fig. 5. Summary of the T_0 of current main strain glass alloy systems. The data of Ti–Ni-based strain glasses come from Refs. [6,12,19,20], the data of Ti–Pd-based strain glasses are from Ref. [13], and the data of ferromagnetic strain glass alloys come from Refs. [10,20,21].

These two new strain glass systems exhibit a relatively high ideal freezing temperature T_0, as compared with other systems. Figure 5 summarizes the T_0 of current main strain glass systems. In Ti–Ni-based strain glass alloys, T_0 is generally lower than 200 K.[6,12,19,20] Ti–Pd-based strain glass alloys exhibit a relatively high T_0, which is around 250 K.[13] As for the ferromagnetic strain glass (FSTG) alloys, the highest T_0 is also around 250 K.[10,21,22] Thus, the highest T_0 of current strain glass systems is around 250 K. In comparison, the T_0 of the $Ti_{50}Au_{25}Cr_{25}$ strain glass alloy is about 251 K, which is comparable with the highest T_0 value, and that of the $Ti_{50}Pt_{20}Fe_{30}$ strain glass alloy is about 272 K, which is even higher than the T_0 maximum of the current main strain glass alloys.

Although the strain glass in the $Ti_{50}Pt_{20}Fe_{30}$ alloy exhibits the highest T_0 so far, it is not high enough as expected, given that the host alloy $Ti_{50}Pt_{50}$ exhibits a quite high M_s ($\sim$ 1340 K).[2] Figure 6 compares the phase diagrams of several Ti-based alloys.[12,13] The composition dependence of the transformation behavior is similar for these four systems: there is a critical defect concentration separating the martensitic phase and strain glass. It is noted that as the M_s of the host alloy increases, the critical defect concentration strongly increases, whereas the increase of the T_0 is limited. As a result, although the Ti–Pt-based alloys start from the pure $Ti_{50}Pt_{50}$ host alloy with high M_s ($\sim$ 1340 K), much higher than the M_s of the pure $Ti_{50}Pd_{50}$ host alloy ($\sim$ 800 K) in Ti–Pd-based alloys, the T_0 of the strain glass in Ti–Pt-based alloys ($\sim$ 272 K) is only slightly higher than that of the strain glass in Ti–Pd-based alloys ($\sim$ 250 K).

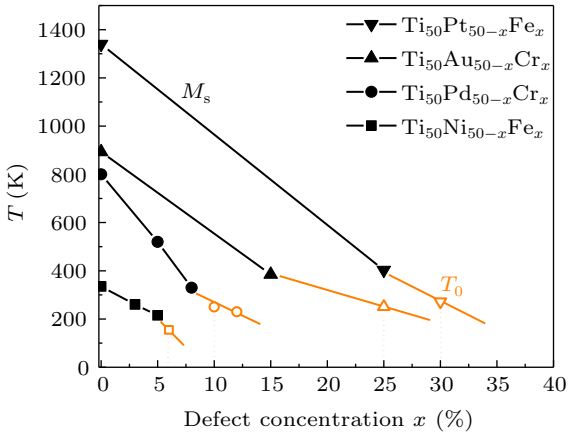

Fig. 6. Comparison of the phase diagrams of Ti-based SMAs. The critical defect concentration for each system is labeled by the red dot line. The data of $Ti_{50}Ni_{50-x}Fe_x$ and $Ti_{50}Pd_{50-x}Cr_x$ come from Refs. [12,13], and the data of $Ti_{50}Pt_{50}$ and $Ti_{50}Au_{50}$ are from Ref. [2].

Obviously, doping point defects is not an effective way to further increase the T_0 of strain glass above ambient temperature. According to the phenomenological model of strain glass,[23] point defects generally introduce two effects to the martensitic system: One is a global effect, which changes the global thermodynamic stability of martensite; the other is a local effect, which leads to a fluctuation in local thermodynamic stability of martensite. In most cases, the global effect of point defects is to decrease the M_s, which causes a strong transition temperature decrease before the system goes to the strain glass and thus results in a low T_0.

Besides the point defects, some other crystallographic defects such as dislocations[24] and nanoprecipitates[25,26] have also been reported to be able to suppress the martensitic transformation and generate a frozen strain glass state. Moreover, it is reported that the dislocations and nanoprecipitates can

maintain the T_0 of strain glass better than the point defects.[24] The reason is that the global effect of dislocations is negligible, while nanoprecipitates sometimes may lead to an opposite global effect as compared with point defects (for example, the M_s of the B2-R martensitic transition in Ti–Ni SMAs increases due to the Ti_3Ni_4 precipitation[5]). Thus, a potential solution to design high T_0 strain glass alloys is to choose a host alloy with high M_s and introduce other defects such as dislocations and nanoprecipitates in it, which requires a further study in the future.

Moreover, in ferromagnetic shape memory alloys which are an important subgroup of SMAs, the global effect of point defects may vary due to the magnetoelastic coupling. For example, in Co-doped Ni–Mn–Ga ferromagnetic strain glass alloys, the M_s first keeps constant rather than decreases with doping cobalt, and the T_0 in this system is actually comparable with that of strain glass in Ti–Pd-based SMAs.[21] Thus, ferromagnetic shape memory alloys are also a promising candidate to exhibit high T_0, worthy to be further investigated.

4. Conclusion

We found high temperature strain glass in Ti–Au-based and Ti–Pt-based HTSMAs. The critical defect concentration for $Ti_{50}Au_{50-x}Cr_x$ alloys is around $x = 25$, while that for $Ti_{50}Pt_{50-y}Fe_y$ alloys is about $y = 30$. The T_0 of strain glass in Ti–Au-based alloys is around 251 K, and that of strain glass in Ti–Pt-based alloys is around 272 K. Both of them are comparable with the highest T_0 value so far. This work suggests that doping point defects is not an effective way to increase the T_0 above the ambient temperature, some other methods are required to find the strain glass with higher T_0.

References

[1] Otsuka K and Wayman CM (eds.) 1998 *Shape Memory Materials* (Cambridge: Cambridge University Press) pp. 1–48

[2] Donkersloot H C and Van Vucht J H N 1970 *J. Less-Common. Met.* **20** 83

[3] Kawamura T, Tachi R, Inamura T, Hosoda H, Wakashima K, Hamada K and Miyazaki S 2006 *Mater. Sci. Eng. A* **438-440** 383

[4] Yamabe-Mitarai Y, Arockiakumar R, Wadood A, Suresh K S, Kitashima T, Hara T, Shimojo M, Tasaki W, Takahashi M, Takahashi S and Hosoda H 2015 *Mater. Today Proc.* **2** S517

[5] Otsuka K and Ren X 2005 *Prog. Mater. Sci.* **50** 511

[6] Sarkar S, Ren X and Otsuka K 2005 *Phys. Rev. Lett.* **95** 205702

[7] Ren X 2014 *Phys. Status Solidi B* **251** 1982

[8] Wang D, Hou S, Wang Y, Ding X D, Ren S, Ren X B and Wang Y Z 2014 *Acta Mater.* **66** 349

[9] Wang Y, Song X P, Ding X D, Yang S, Zhang J, Ren X B and Otsuka K 2011 *Appl. Phys. Lett.* **99** 051905

[10] Ren S, Xue D Z, Ji Y C, Liu X L, Yang S and Ren X B 2017 *Phys. Rev. Lett.* **119** 125701

[11] Wang W H 2019 *Prog. Mater. Sci.* **106** 100561

[12] Wang D, Zhang Z, Zhang J, Zhou Y, Wang Y, Ding X, Wang Y and Ren X 2010 *Acta Mater.* **58** 6206

[13] Zhou Y M, Xue D Z, Ding X D, Otsuka K, Sun J and Ren X B 2014 *Phys. Status Solidi B* **251** 2027

[14] Zhang Z, Wang Y, Wang D, Zhou Y M, Otsuka K and Ren X B 2010 *Phys. Rev. B* **81** 224102

[15] Vasseur R, Xue D Z, Zhou Y M, Ettoumi W, Ding X D, Ren X B and Lookman T 2012 *Phys. Rev. B* **86** 184103

[16] Liang Q L, Wang D, Zhang J, Ji YC, Ding X D, Wang Y, Ren X B and Wang Y Z 2017 *Phys. Rev. Mater.* **1** 033608

[17] Zhang J, Wang Y, Ding X D, Zhang Z, Zhou Y M, Ren X B, Wang D, Ji Y C, Song M H, Otsuka K and Sun J 2011 *Phys. Rev. B* **84** 214201

[18] Wang Y, Huang C H, Wu H J, Gao J H, Yang S, Wang D, Ding X D, Song X P and Ren X B 2013 *Appl. Phys. Lett.* **102** 141909

[19] Ren S, Zhou C, Xue D Z, Wang D, Zhang J, Ding X D, Otsuka K and Ren X B 2016 *Phys. Rev. B* **94** 214112

[20] Zhou YM, Xue D Z, Ding X D, Wang Y, Zhang J, Zhang Z, Wang D, Otsuka K, Sun J and Ren X B 2010 *Acta Mater.* **58** 5433

[21] Wang Y, Huang C H, Gao J H, Yang S, Ding X, Song X and Ren X 2012 *Appl. Phys. Lett.* **101** 101913

[22] Monroe J A, Raymond J E, Xu X, Nagasako M, Kaimuma R, Chumlyakov Y I, Arroyave R and Karaman I 2015 *Acta Mater.* **101** 107

[23] Wang D, Wang Y Z, Zhang Z and Ren X B 2010 *Phys. Rev. Lett.* **105** 205702

[24] Zhang J, Xue D Z, Cai X Y, Ding X D, Ren X B and Sun J 2016 *Acta Mater.* **120** 130

[25] Ji Y C, Ding X D, Lookman T, Otsuka K and Ren X B 2013 *Phys. Rev. B* **87** 104110

[26] Ren S, Liu C, Chen X, Hao Y S and Ren X B 2020 *Scr. Mater.* **177** 11